Journal of the Korean Physical Society (2023) 82:236–243
https://doi.org/10.1007/s40042-022-00661-1

Online ISSN 1976-8524
Print ISSN 0374-4884

ORIGINAL PAPER - PARTICLES AND NUCLEI


# FPGA-based trapezoidal digital pulse shaping in nuclear spectrometry

**Hyojeong Choi**[1] · **Jong-Seo Chai**[1]

Received: 1 September 2022 / Revised: 4 October 2022 / Accepted: 13 October 2022 / Published online: 10 January 2023


**Abstract**
A digital pulse processing is most widely used in nuclear spectrometry for achieving good energy resolution at high count rates. We developed a digital pulse processing system to implement a peak detection algorithm using digital trapezoidal pulse shaping. The incident radiation signal amplified by the preamplifier is converted into digital data through the prefilter and the analog-to-digital converter; then, this signal is shaped into trapezoidal pulses through the implemented algorithm which consists of rising edge detection, pile-up signal discrimination and offset remove, two stages of convolutions, peak detection and ballistic deficit discrimination. We compared a linearity of the system between simulation and experimental results. The noise was calculated using a commercial test input pulser, and then, the 59.5 keV of gamma-ray spectrum with CdTe Schottky detector was obtained using an Am-241 radioisotope source. This system showed better noise characteristics and gamma-ray spectroscopy characteristics than existing commercial analog systems.

**Keywords** Digital pulse processing · Trapezoidal shaping · Radiation detection

## 1 Introduction

Owing to the advent of high-speed analog-to-digital converters (ADCs) and the development of field-programmable gate arrays (FPGAs), it is possible to adjust the shaping parameters in real time by considering the characteristics of the generated signal and improving the throughput performance [1]. FPGA-based digital signal processing techniques are being widely studied in nuclear spectroscopy to achieve high resolution and throughput of incident radiation. After the radiation is incident on the detector, the output signal from the preamplifier with R–C feedback connected to this detector has a short rise time of several tens to hundreds of nanoseconds and a long falling time of several hundred microseconds. In the case of digital signal processing, the most commonly used shaping method to increase the signal-to-noise (S/N) ratio of this preamplifier output signal is trapezoidal pulse shaping, and research on triangular and digital Gaussian shaping is being actively conducted [2–5]. Because it is difficult to generate trapezoidal pulse shapes in analog shaping circuits, semi-Gaussian shaped pulse shaping is mainly performed. Theoretically, the S/N ratio of a trapezoidal pulse is higher than that of the semi-Gaussian pulse [2]. Although triangular pulses show superior FWHM compared to trapezoidal pulses, it is important to use trapezoidal pulses to eliminate ballistic deficits when detecting radiation using a detector with a slow charge collection time such as CdTe. In an ideal case, when radiation is incident on the detector, a step signal with a rising time of 0 of the preamplifier output signal should occur; however, a ballistic deficit inevitably occurs owing to the finite charge collection time. In addition, the output signal of the charge-sensitive preamplifier increases exponentially with the rising edge owing to the CR component of the preamplifier, which can be expressed by uni-exponential and bi-exponential functions [6]. If digital pulse shaping is performed using the Z-transform technique based on this signal, amplitude reduction due to a ballistic deficit and distortion of the shaping output pulse due to parameter drift occur. In conclusion, the existing digital pulse processing technique, especially trapezoidal pulse shaping, must secure a sufficient flat-top length to eliminate the effect of ballistic deficit and correct the distortion caused by parameter drift. If the effect of the ballistic deficit is not considered, the flat-top shaped trapezoidal pulse does not exhibit an amplitude proportional to the incident radiation energy. This results in inhibiting the linearity of the output signal and increasing the FWHM in

✉ Jong-Seo Chai
jschai@skku.edu

[1] College of Information and Communication Engineering, Sungkyunkwan University, Suwon 16419, Republic of Korea

the radiation response. Additionally, this in turn leads to an increase in the pulse processing time. To solve this problem, advanced digital pulse processing algorithms [1, 7, 8] related to adaptive digital pulse shaping that adjust the coefficients in real time to shape an input signal into a desired output signal are being developed. Recursive algorithm is the most commonly used to implement digital pulse processing, which allows the pulse shaping with less resources and performs pulse shaping quickly. Through this, it is possible to more effectively reduce the pile-up in an environment with a high counting rate and to optimize the time constant of the pulse to obtain a high S/N ratio.

The analog prefilter output signals enter the digital pulse processor through an ADC. In this study, a digital pulse processor using the designed analog prefilter output signal was implemented using a convolution algorithm. The purpose of using the convolution algorithm is to convert the analog prefilter signal into a trapezoidal shape so that the incident X-ray energy information can be obtained. This shaping method is effective for determining the maximum amplitude with a high S/N ratio [9, 10] from the bi-exponential input signal, that is, prefilter output pulse.

## 2 System design

Figure 1 shows a flowchart of the design, which is called the peak-detection algorithm. Unlike other trapezoidal shaping algorithm, it performs the convolution in two steps, such as step signal shaping and trapezoidal signal shaping. Converting the step signal into a trapezoidal shape can provide accurate flat-top than using the bi-exponential signal, which is usual preamplifier output. First, analog signals from the prefilter output are digitized using a 14-bit ADC. The desired pulse is detected in real time using rising edge detection. When a rising edge is detected, the trigger starts and holds the signal. In the next stage, the pile-up signal discriminator determines whether the signal is piled-up. If it is, the input signal buffers are removed and returned to rising edge detection. Because the designed convolution algorithm is a method for calculating the area of the input signals, the piled-up signal causes a distortion of the spectrum. If the input pulse is collected in working order, the DC offset is removed. Thereafter, the first convolution is performed. The output signal to this stage has a saw-tooth shape. The purpose of this process is to create an ideal trapezoidal signal. Consequently, the output is generated with a constant slope and different amplitudes, which relies on the amplitude of the analog input. The second convolution, called

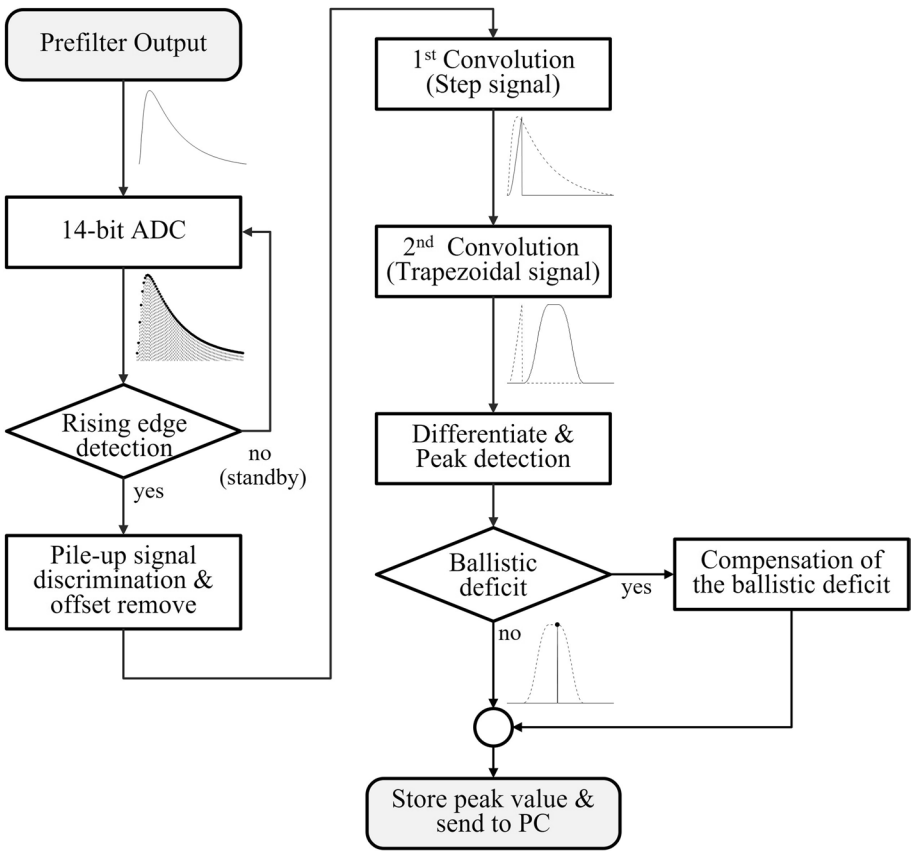


**Fig. 1** Flowchart of the peak detection algorithm

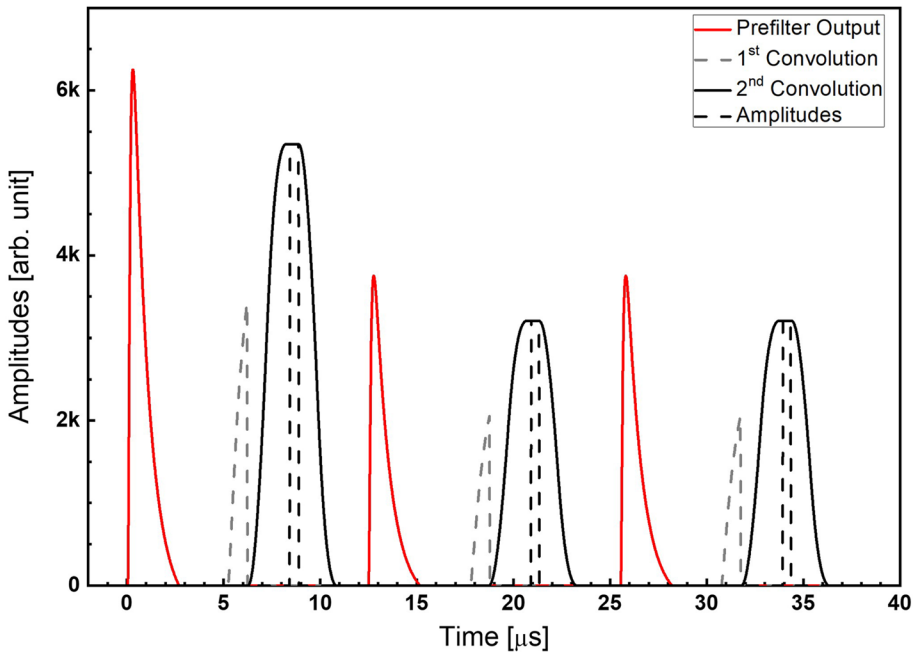


**Fig. 2** ISIM simulation results of prefilter output (red solid line), first convolution (gray solid line), second convolution (black solid line) and amplitudes of the trapezoidal pulse (black-dashed line)

trapezoidal convolution, is performed on the output of the first convolution process. The flat-top amplitude of the trapezoidal signal is directly related to the incident X-ray energy. From the trapezoidal signal, the ballistic deficit should be distinguished [11, 12]. If the rise time of the input signal is zero, ballistic deficit does not occur. However, in practice, the rise edge increases exponentially. Therefore, it should be distinguished and removed so that the peak value is not distorted. To discriminate the ballistic deficit, differentiation is performed within the flat-top period. If a '0' value can be obtained by differentiation, actual flat-top amplitudes can be determined at this period. The peak value for each pulse is transferred to a PC with RS-232 serial communication.

Verilog code was used to implement the digital pulse processing system. The convolution algorithm was coded based on Eqs. (1) and (2).

$$
\begin{aligned}
&c_1(0) = v(0)\\
&c_1(n) = c_1(n-1) + v(n), (0 < n \le k-1)\\
&c_1(n) = c_1(n-1), (k \le n \le l-1)\\
&c_2(0) = c_1(0)\\
&c_2(n) = c_2(n-1) + c_1(n), (0 < n \le k-1)\\
&c_2(n) = c_2(n-1) + c_1(n) - c_1(n-k), (k \le n \le k+m-1)\\
&c_2(n) = c_2(n-1) + c_1(n) - c_1(n-k)\\
&\qquad - c_1(n-k-m), (k+m \le n \le l-1)
\end{aligned}
\tag{1}
$$

$$
\begin{aligned}
c_2(n) =& c_2(n-1) + c_1(n) - c_1(n-k)\\
&- c_1(n-k-m) + c_1(n-1),\\
&(l \le n \le l+b)
\end{aligned}
\tag{2}
$$

where $v(n)$ is the input signal, $c_1(n)$ is the first convolution signal, $c_2(n)$ is the second convolution signal, $k$ is the rise period, $m$ is the flat-top period and $l$ is the total length $(2 \times k + m)$. For the generating symmetric trapezoidal pulse, period of coefficients to produce rising and falling time of trapezoidal pulse should be same as time constant of prefilter output. Digital pulse processor with a peak detection algorithm was operated at a frequency of 50 MHz, and total number used as logic and exclusive route-thru in our implemented FPGA design was 2561 and 8, respectively. Additionally, total number used as flip-flops was 1007.

## 3 Simulations and experiments set-up

The designed algorithm was simulated using an ISE simulator(ISim) simulator supported by Xilinx® [13]. Figure 2 shows the simulation results of the prefilter, first and second convolution, and amplitudes of the trapezoidal pulses.

A prefilter was designed to remove the pile-up signal, which may occur. Therefore, the pile-up rejection was implemented using digital pulse processing. This is referred to as the pile-up signal discrimination, as shown in Fig. 1. From

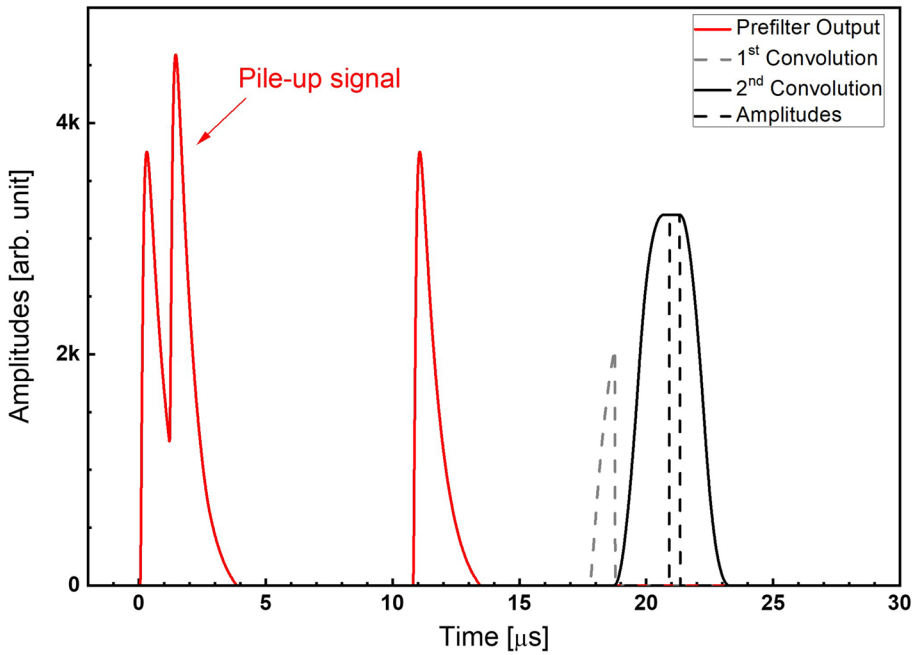


**Fig. 3** Simulation result of the pile-up discrimination. A pile-up signal is ignored to perform trapezoidal pulse shaping

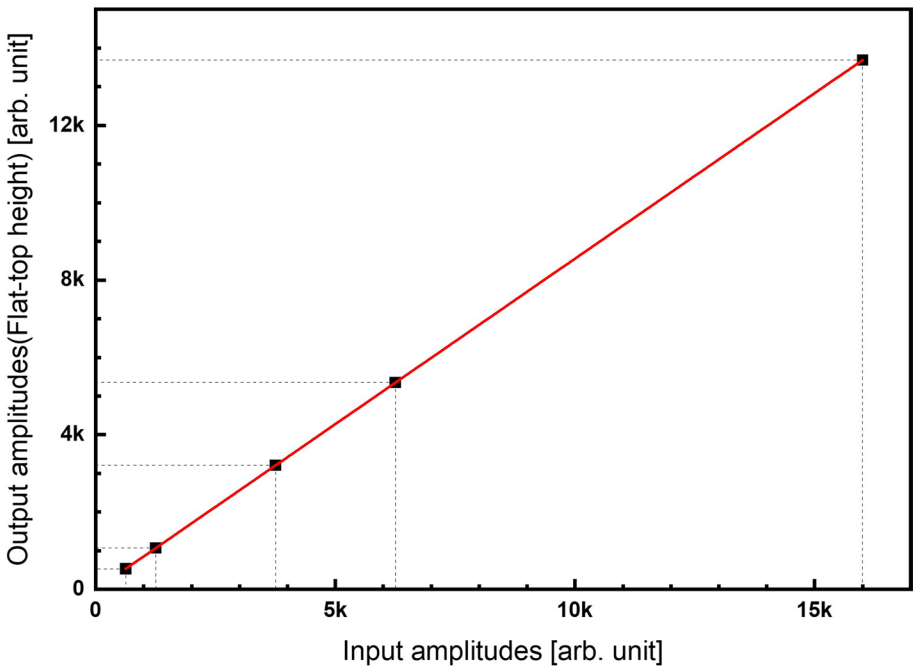


**Fig. 4** Linearity simulation results of input amplitudes versus output amplitudes. A slope of the linear curve is 0.85

the simulation, convolution did not proceed when the pile-up signal entered into the digital pulse processor, as shown in Fig. 3.

From the simulation results, the flat-top heights of the trapezoidal signals were proportional to the input pulse amplitudes, with a slope of 0.85, as shown in Fig. 4. Linearity is an important property of the implemented systems. To match the value between output and input amplitudes, the flat-top height should be divided by the coefficient. The different slopes originate from this coefficient, which can be used for digital gain.

The experimental set-up used to verify the designed algorithm is illustrated in Fig. 5. The system consisted of an Ortec 419 precision pulse generator that can adjust the rise time of the pulse from 5- to 250-ns, an eV-5091 preamplifier by eVProducts, an analog prefilter, a DSP-PLUS II FPGA development kit including XC5VSX95T-1FF1136 Virtex-V FPGA, and data acquisition software. The implemented

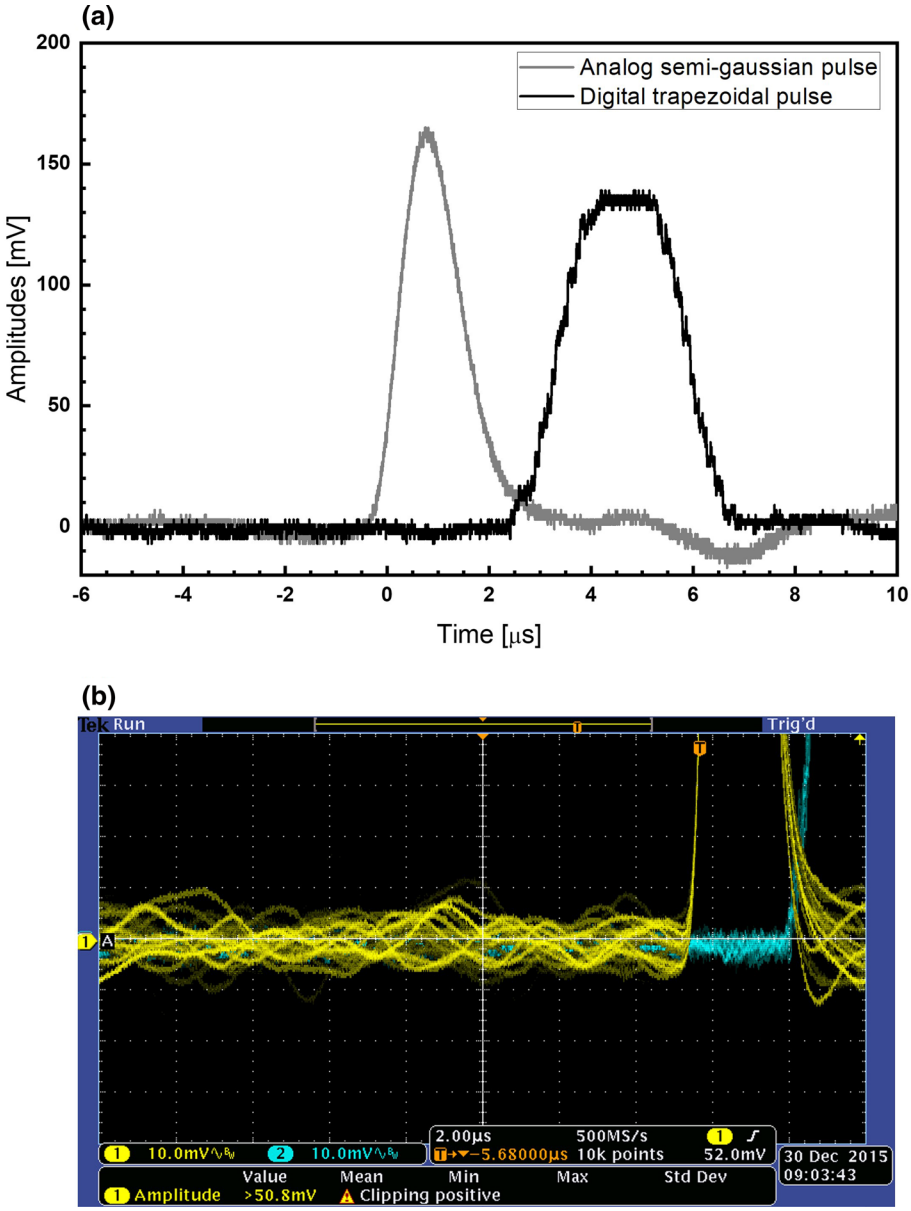


**Fig. 5** **a** Comparison between the waveforms of digital trapezoidal pulse (black solid line) and analog semi-Gaussian pulse (gray solid line). **b** Comparison between the baseline of digital trapezoidal pulse (blue line) and analog semi-Gaussian pulse (yellow line)

Verilog code was programmed into the Virtex-5 FPGA in the DSP-PLUS II FPGA development kit. The prefilter output was digitized using a 14-bit ADC which is an ADS5422 by Texas Instruments and has a maximum sampling rate of 62 mega sampling per second. Then digitized values were processed using the designed peak detection algorithm. An investigation of prefilter's role and performance were reported in Reference [14]. Finally, trapezoidal-shape pulses were converted using DAC and observed by oscilloscope.

To compare the properties such as noise and gamma response, the implemented digital pulse processing system and conventional analog pulse processing system were set. An analog pulse processing system was composed of eV5093 preamplifier, Ortec 572A shaping amplifier, Ortec 928 MCA and Ortec Maestro software.

## 4 Results and discussions

Figure 5 shows a trapezoidal pulse and semi-Gaussian pulse observed by an oscilloscope. Each shaped pulse is shown in Fig. 5a, and baseline vibrations of both pulses were captured by oscilloscope, as shown in Fig. 5b. Peak-to-peak voltages of the baseline of digital shaped pulse and analog shaped pulse were 8 and 18 mV, respectively.

In digital shaping, the response goes to zero immediately after finishing a period of shaping. However, in analog shaping, if large numbers of radiation events occur, as used for semiconductor detectors with high-atomic number, there is not enough time to go to baseline. This is because the tail of the shaped signal requires infinite time to go to the baseline. Therefore, a digital pulse processor can improve the

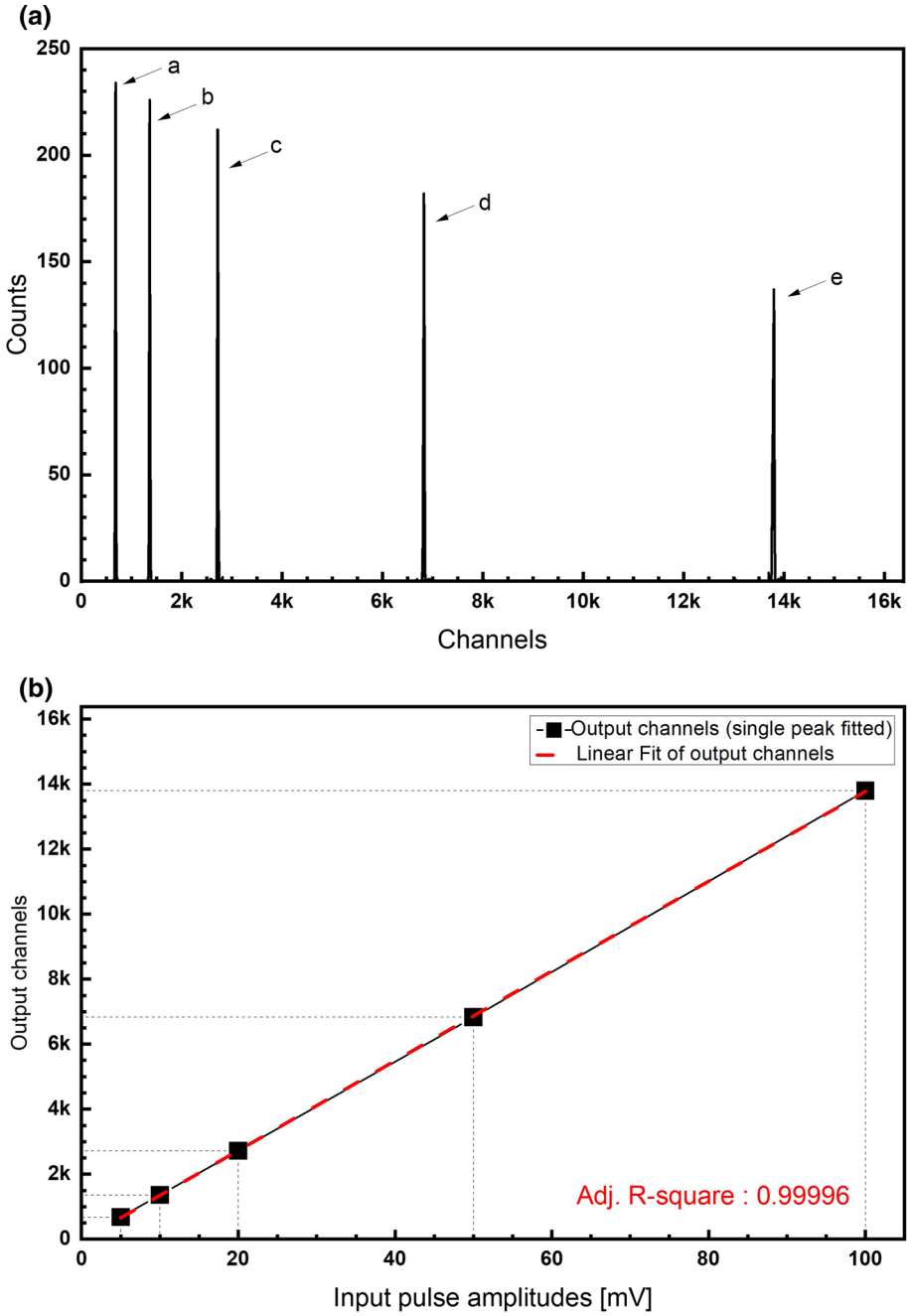


**Fig. 6** **a** Output spectra obtained by proposed digital pulse processing system according to the amplitudes of input pulses (a: 5 mV, b: 10 mV, c: 20 mV, d: 50 mV, e: 100 mV). **b** Linearity calculation results by obtained spectra. A red-dashed line is fitted curve of output pulses

performance, such as reducing the pile-up and baseline shifts at high count rates. Another advantage of using a digital shaper is that digital shaping can easily tailor the needs of an application by changing the choice of the integer parameter. However, it is limited in analog systems because they rely on resistors and capacitors to change the parameters, such as the shaping time.

As mentioned above, the linearity of the output signal with respect to the input signal is an important characteristic of the system. The output spectra shown in Fig. 6a were obtained using test input pulses with amplitudes of 5, 10, 20, 50, and 100 mV.

The center of each peak, which was calculated by single peak fitting, was fitted by linear fitting (Fig. 6b). From the fitting, a high-adjusted *R*-value of 0.99996 was calculated. It can be confirmed that experimental results were well matched with simulation results, as shown in Fig. 4, and the linearity of this system is guaranteed.

Figure 7 shows the spectral results of the prefilter and Ortec 572A. In both cases, input pulse amplitude and rise

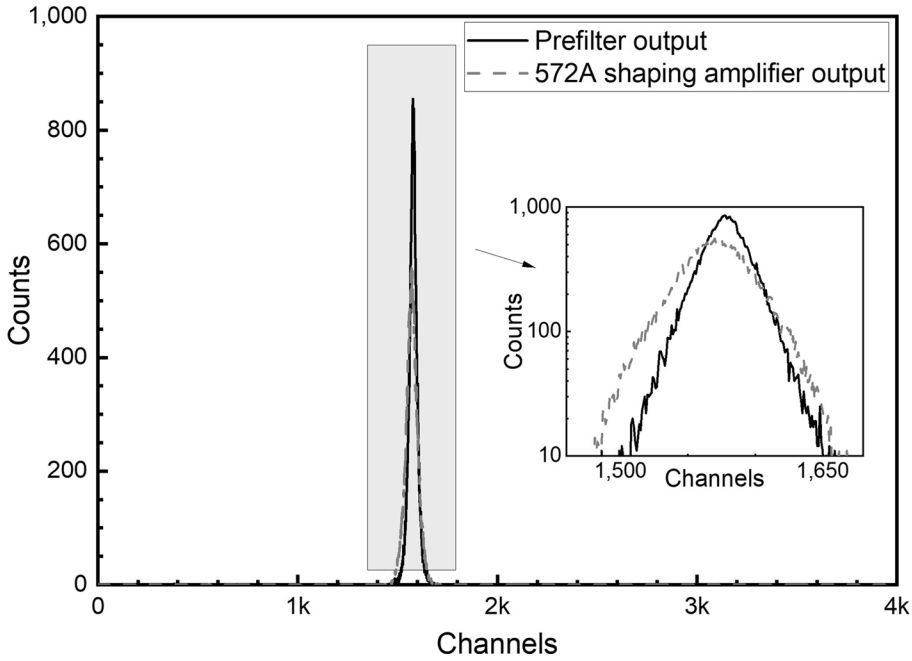


**Fig. 7** Noise properties of a prefilter output and an Ortec 572A shaping amplifier output with 10 mV test pulse input

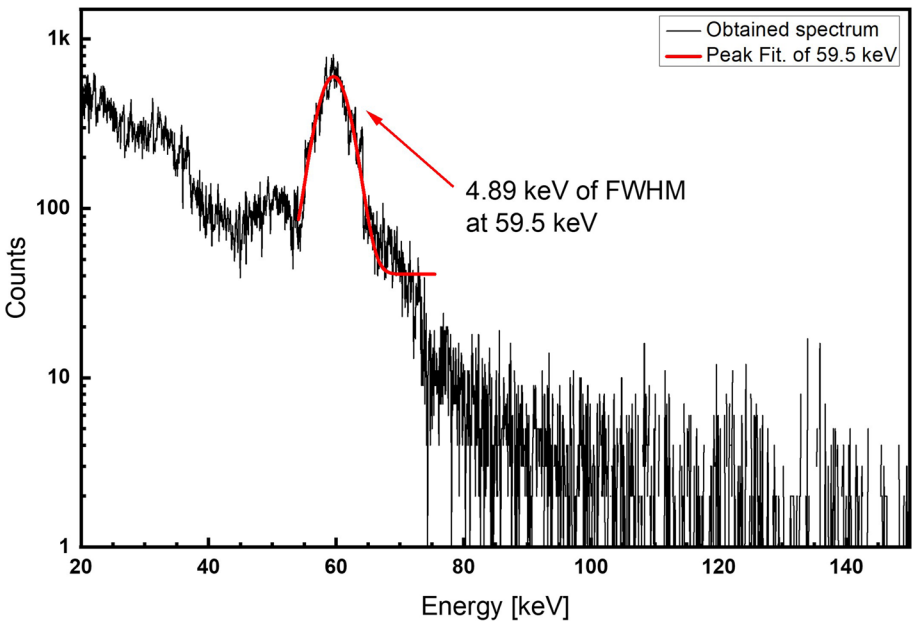


**Fig. 8** 59.5 keV of gamma-ray energy spectrum obtained using Am-241 radioisotope

time were 10 mV and 200 ns, respectively. The measurement time was 120 s.

As determined by calculating the FWHM of spectra, the FWHM of the prefilter was 2.1% and that of the 572A shaping amplifier was 3.43%. Both of FWHMs were obtained by single peak fitting. This value is not absolutely applicable to the prefilter or shaping amplifier, but is the sum of the total noise generated by the pulser, preamplifier, and MCA. It was proven that the noise of the system equipped with the prefilter was superior to that of the 572A shaping amplifier. However, when the pulse rise time was set to the least possible value, such as 50 ns, the 572A shaping amplifier showed slightly better performance; 2.2% for the prefilter and 1.8% for the 572A shaping amplifier.

Finally, the radiation spectrum was measured using Am-241 radioisotope. The test environment was the same as in the above experiments, but a CdTe Schottky diode biased at − 700 V was mounted on a PCB board instead of an input pulser. The spectrum was obtained over 3600 s. The spectrum obtained is shown in Fig. 8.

**Table 1** FWHM and Adj. *R*-square at 59.5 keV of gamma-ray energy for the implemented digital pulse processing system and commercial analog pulse processing system

| | FWHM (keV) | Adj. *R*-square |
|---|---|---|
| Implemented digital pulse processing system | 4.89 | 0.93116 |
| Commercial analog pulse processing system | 5.71 | 0.98594 |

Adj. *R*-squares were calculated after single peak fitting by Origin software. Adj. *R*-square is more accurate than simple *R*-square when the predictable numbers are different [15]

At 59.5 keV of gamma-ray energy, 4.89 keV of FWHM from single peak fitting was obtained. In contrast to the test input pulse, signals from the incident radiation are produced randomly. In addition, various amplitudes of the produced signals were observed. The results obtained using the radioisotope source and CdTe detector indicate that these signal processors can operate well with radiation measurements. Furthermore, 59.5 keV of gamma-ray energy spectrum with 5.71 keV of FWHM was also obtained using an analog pulse processing system. The implemented digital pulse processing system showed better FWHM than that of an analog pulse processing system because ballistic deficit was eliminated by trapezoidal pulse shaping. The FWHM results are presented in Table 1.

## 5 Conclusion

In this study, the properties of digital pulse processing are provided. Digital pulse processing has some obvious advantages such as low electronic noise and baseline distortion compared to analog pulse processing. The experimental results in our implemented system showed that FWHM of the gamma-ray response can be reduced using a simple peak detection algorithm. It was proved that this system is effective for a semiconductor detector with a relatively slow rise time such as CdTe; however, this system exhibited lower performance than the analog pulse processing system when the rise time of the input pulse was less than 200 ns, since the flat-top length was set long enough to eliminate the ballistic deficit. In other words, parallel noise was increased as the flat-top length increased. A further study that flat-top length is adjustable in real time according to the rise time of the pulse is needed.

**Acknowledgements** This work was supported by the Korea Medical Device Development Fund grant funded by the Korea government (the Ministry of Science and ICT) (Project Number: 1711135001, KMDF_PR_20200901_0042). This work was also supported by the Korea Atomic Energy Research Institute Internal Project (523510-22, 523160-22) and K-sensor development project (RS-2022-00144108)

## References

1. S. Saxena, A.I. Hawari, IEEE Trans. Nucl. Sci. **64**, 1733 (2017)
2. V.T. Jordanov, G.F. Knoll, F.K. Glenn, Nucl. Instrum. Methods Phys. Res. A **345**, 337 (1994)
3. M. Nakhostin, IEEE Trans. Nucl. Sci. **58**, 2378 (2011)
4. Z. Jianbin et al., Nucl. Sci. Tech. **23**, 150 (2012)
5. Z. Guzik, T. Krakowski, Nukleonika **58**, 333 (2013)
6. S. Wengang, Z. Lijun, W. Guanying, IEEE Trans. Nucl. Sci. **67**, 1710 (2020)
7. A. Regadio, S. Sanchez-Prieto, M. Prieto, J. Tabero, Nucl. Instrum. Methods Phys. Res. A **735**, 297 (2014)
8. S. Saxena, A.I. Hawari, Nucl. Instrum. Methods Phys. Res. A **954**, 161288 (2020)
9. F.S. Goulding, Nucl. Instrum. Methods **100**, 493 (1972)
10. C. Imperiale, A. Imperiale, Measurement **30**, 49 (2001)
11. S.M. Hinshaw, D.A. Landis, IEEE Trans. Nucl. Sci. **37**, 374 (1990)
12. K. Hatch, IEEE Trans. Nucl. Sci. **15**, 303 (1968)
13. https://www.xilinx.com/products/design-tools/isim.html.
14. H. Choi et al., J. Korean Phys. Soc. **69**, 1157 (2016)
15. https://www.originlab.com/doc/Origin-Help/Interpret-Regression-Result#Adj._R-Square